치의과학박사 학위논문

# Exploration of measurement of conditions for three-dimensional bone-to-implant contact ratio using micro-computed tomography and comparison with histological approach

## 마이크로 전산화 단층촬영을 이용한 3 차원 골-임플란트 접촉률 측정 조건 탐색과 조직학적 측정법과의 비교

2023 년 8 월


서울대학교 대학원

치의과학과 치과보철학 전공

홍 정 민

# Exploration of measurement of conditions for three-dimensional bone-to-implant contact ratio using micro-computed tomography and comparison with histological approach

지도교수 여 인 성

이 논문을 홍정민 박사학위논문으로 제출함

**2023** 년 **6** 월

서울대학교 대학원

치의과학과 치과보철학 전공

홍 정 민

홍정민의 박사학위논문을 인준함

**2023** 년 **7** 월

위 원 장 _____ (인)

부 위 원 장 _____ (인)

위 원 _____ (인)

위 원 _____ (인)

위 원 _____ (인)

**- ABSTRACT -**

# Exploration of measurement of conditions for three-dimensional bone-to-implant contact ratio using micro-computed tomography and comparison with histological approach

**Jeong-Min Hong,** D.D.S., M.S.D.

*Department of Prosthodontics, Graduate School, Seoul National University*

*(Directed by Professor In-Sung Yeo, D.D.S., M.S.D., Ph.D.)*

***Purpose*:** Histological analysis is widely regarded as the gold standard method of evaluating osseointegration around a bone-implant. However, this approach requires invasive specimen preparation and is limited to representing only a single plane. By comparison, micro-computed tomography (μCT) offers a rapid and convenient alternative that provides three-dimensional information, but is hampered by resolution and artifacts-related issue, making it a supplementary method for osseointegration analysis. To verify the reliability of μCT for osseointegration evaluation, this animal model study compared bone-to-implant contact (BIC) ratios obtained by the gold standard histomorphometric method with those obtained by the μCT method, using a rabbit tibia implant model.

***Materials and methods*:** A sandblasted, large-grit, acid-etched (SLA) implant and a machined surface implant were inserted into each tibia of two rabbits (giving eight implants in total). Bone-implant specimens were analyzed using μCT with a spiral scan technique (SkyScan 1275) and histological sections were prepared thereafter. Three-dimensional (3D) reconstructed μCT data and four two-dimensional (2D) μCT sections, including one section corresponding to the histologic section and three additional sections rotated 45°, 90°, and 135°, were used to calculate the BIC ratio. The Pearson's test was used for correlation analysis at a significance level of 0.05.

***Results*:** The histomorphometric BIC and the 2D-μCT BIC showed strong correlation ($r = 0.762$, $P = 0.046$), whereas the histomorphometric BIC and 3D-μCT BIC did not ($r = -0.375$, $P = 0.385$). However, the mean BIC value of three or four 2D-μCT sections showed a strong correlation with the 3D-μCT BIC (three sections: $r = 0.781$, $P = 0.038$; four sections: $r = 0.804$, $P = 0.029$).

***Conclusion*:** The results of this animal model study indicate that μCT can serve as a valuable complement to the histomorphometric method for bone-implant interface analyses. With the limitations of this study, 3D-μCT analysis may even have a superior aspect by eliminating random variables that can arise as a consequence of the selected cutting direction.

**Key words**: Bone-implant interface, osseointegration, Bone-to-implant contact ratio, micro-CT analysis, dental implant

**Student Number**: 2018-30905

# CONTENTS

# I. BACKGROUND

Bone responses to dental implants are commonly evaluated through quantitative analyses of direct bone-to-implant contact (BIC), also known as osseointegration (Albrektsson et al, 1981, Johansson and Albrektsson, 1991). Osseointegration is essential for the successful clinical outcome of dental implants, which is assessed based on criteria such as stability, functionality, and maintenance (Sennerby et al, 2001). A strong and intimate interface between the implant and the surrounding bone ensures efficient transfer of occlusal forces, thus enabling the implant to withstand masticatory loads and function akin to a natural tooth. Since the introduction of the concept of osseointegration by Brånemark in 1977, measurement of the BIC ratio on an undecalcified histological section using light microscopy has been regarded as the gold standard analysis method (Brånemark, 1977, Brånemark, 1983, Brånemark et al, 2001, Stadlinger et al, 2007). This histomorphometrical method provides qualitative information as well as quantitative analysis, such as the presence and organization of cells around the implant, indicating the status of inflammation, remodeling, and regeneration of the bone tissue.

Despite providing valuable qualitative information as well as quantitative ones, this histomorphometric approach is inherently destructive and time-consuming. It necessitates intensive preparation procedures such as sawing, grinding, and staining of the bone-implant section, all of which can potentially result in technical errors (Sprecher et al, 2013). The invasiveness of the procedure also damages the specimen, precluding further examination, and does not allow evaluation of the specimen at various time

points (Müller et al, 1998, Gao et al, 2009). Histomorphometric analyses also have the crucial drawback that only a small number of two-dimensional (2D) sections with the same orientation can be made; consequently, there is uncertainty over whether this method of measurement accurately represents the entire three-dimensional (3D) bone-to-implant surface. Therefore, despite the reliability of the histomorphometric method, a convenient and objective technique that allows 3D analysis of the BIC is needed.

Recently, micro-computed tomography (μCT) has emerged as a potential alternative method to assess the 3D morphology and architecture of BICs (Palmquist et al, 2017, Jimbo et al, 2011). This non-destructive and fast method offers not only information about the 3D structure, but can also be used to assess quantitative parameters such as bone density (Al Subaie et al, 2015, Becker et al, 2015). The drawback of μCT is that it has a lower resolution than light microscopy, causes the partial volume effect (PVE), and creates artifacts that can obstruct evaluation of the implant surface (Boas and Fleischmann, 2012, Stoppie et al, 2005). PVE refers to a phenomenon that occurs in imaging techniques, such as μCT, where the resolution of the imaging system is insufficient to accurately represent small structures or boundaries. It occurs when a voxel contains a mixture of different materials or tissues with varying densities such as bone, soft tissue, and air, for example. As a result, the boundaries between these different materials may appear blurred or indistinct, leading to inaccuracies in quantifying their individual properties, particularly relevant when analyzing structures with fine details or small features, such as bone-implant interfaces in dental implants. Metal induced artifacts cause more complicated problems in that dental implants have a thread type geometry in addition to the problem that they are made of titanium. To avoid such

problems, a few groups have suggested analyzing the implant surface a few voxels away from the bone interface using μCT (Butz et al, 2006, Bernhardt et al, 2012, Liu et al, 2012, Vandeweghe et al, 2013, Bissinger et al, 2017). In addition, some studies have focused on identifying the optimum conditions for scanning, along with ways to minimize the occurrence of artifacts (de Faria Vasconcelos et al, 2017, Van Oosterwyck et al, 2000, Li et al, 2014, Meagher et al, 2018). Despite these efforts, the limitations of 3D-μCT have not been addressed fully and data generated using this method are currently only used to supplement conventional histomorphometric data (Becker et al, 2015).

Several studies have attempted to assess the consistency between 3D-μCT data and 2D histomorphometric data, but many still show conflicting results; moreover, the conditions for each study, such as the type of μCT device and analysis algorithm, were not standardized (Rebaudi et al, 2004, Liu et al, 2012, Vandeweghe et al, 2013, Bissinger et al, 2017, Schouten et al, 2009, Choi et al, 2019). Accurate verification of the reliability of 3D-μCT data requires a number of criteria to be met: first, the 2D-μCT section corresponding to the histologic section must be defined exactly; second, optimized conditions for BIC analysis, such as segmentation threshold and region of interest (ROI), should be established by comparing the corresponding sections; and third, the BIC analysis of the reconstructed 3D-μCT data must be conducted under these conditions using an appropriate algorithm. To date, only a few studies have performed these three processes. One study suggested that three to four histologic sections, the maximum number that can be obtained along the longitudinal axis of one implant, are sufficient to represent the 3D osseointegration status (Bernhardt et al, 2012). However, only a few

studies have considered the impact of various cutting directions on μCT results (Park et al, 2005, Sarve et al, 2011).

# II. INTRODUNCTION

Implant surface analysis based on μCT has several advantages including multifaceted and automated analyses through 3D reconstruction. However, the BIC analysis method using uCT used in various papers is not standardized. Even in the paper to verify the analysis method using uCT, the standardization of the method is not dealt with. For standardizing through accurate verification, it is also necessary to consider the methodology for each step. Finding the 3D-μCT data that correspond to a specific histologic section, which is starting point to verify the μCT method, have a marked effect on the results. Then, reconstruction of the 3D data set and bone and implant thresholding, must be decided in consideration of in vivo exam and μCT scanning settings. Then proper algorithm should be established for BIC analysis.

The primary aim of this animal model study was to verify the suitability of the 3D-μCT BIC analysis method for osseointegration assessment by comparing it to the histologic BIC analysis method. For validation purposes, we performed an exploration to determine the optimal conditions for 3D-μCT analysis. Titanium implants with two different surfaces were implanted into the tibiae of two rabbits, and a spiral scanning technique, which is known to reduce artifacts associated with screw-shaped dental implants (Choi et al, 2018), was used to generate μCT images. Thereafter, histomorphometric BIC ratios were compared to the BIC ratios of the 2D-uCT sections that matched histologic sections, as well as the BIC ratios of reconstructed 3D uCT data. Additionally, the correlation between the BIC ratios of the 2D-μCT sections generated in variable cutting directions and reconstructed 3D uCT data was compared. The main

alternative hypothesis of this study is that measuring bone-to-implant contact on the direct surface of implants using 3D-μCT is challenging compared to the histological method, even under appropriate conditions. The second alternative hypothesis posits that the utilization of 3D-μCT for measuring bone-to-implant contact can reduce the influence of randomness resulting from the selection of cutting direction.

# III. MATERIALS AND METHODS

## 1. Specimen preparation and in vivo implant surgery

Eight threaded titanium implants (Deep Implant Systems, Seongnam, Korea) were prepared for in vivo surgery, with four implants having a machined surface (turned) and the remaining four were sandblasted, large-grit, acid-etched (SLA) surface implants. These implants had a diameter of 3.4 mm and a length of 12 mm, and were fabricated from grade 4 commercially pure titanium. A notch was created on the top of each fixture using a diamond bur to enable identification of an identical plane between the histomorphometric slide and μCT scan data.

Eight implants were inserted into the tibiae of two normal male New Zealand White rabbits, which were aged between 3 to 4 months, weighed 2.5 to 3 kg, and showed no signs of disease. The animal study protocol was approved by the Ethics Committee of the Animal Experimentation of the Institutional Animal Care and Use Committee (CRONEXIACUC 202103007; Cronex, Hwasung, Korea) and was performed in accordance with the Animal Research: Reporting of In Vivo Experiments (ARRIVE) guidelines (Kilkenny et al, 2012).

The rabbits were anesthetized via intramuscular injection of tiletamine/zolazepam (15 mg/kg, Zoletil® 50, Virbac Korea Co. Ltd., Seoul, Korea) and xylazine (5 mg/kg, Rompun™, Bayer Korea Ltd., Seoul, Korea). Prior to the surgery, the skin on the surgical site was shaved and disinfected with betadine, and then the rabbits were given an intramuscular administration of the antibiotic cephalosporin (Cefazolin; Yuhan Co.,

Seoul, Korea). Each tibia was then locally injected with 0.9 mL of 2% lidocaine with 1:100,000 epinephrine (2% Lidocaine HCL Injection, Huons Co., Ltd, Seongnam, Korea). For implant placement, muscle dissection and periosteal elevation were performed after skin incision to expose the flat surfaces of the tibiae. Drilling was performed mono-cortically under saline irrigation with a final diameter of 3 mm, according to the protocol provided by the implant manufacturer. After bone preparation, two implants were placed in each tibia, resulting in a total of four implants per rabbit. Each implant was placed to make that the marked notch perpendicular to the long axis of the tibia (Johansson and Morberg, 1995). SLA and turned surface implants were arranged in a 2 × 2 Latin square design to ensure complete randomization with minimal sample size (Fig 1). Healing abutments were screwed in after implant placement and the muscle and periosteum were sutured with resorbable 4-0 Vicryl (Ethicon, Somerville, NJ, USA), while the skin was closed using 4-0 blue nylon (Ailee, Busan, Korea). Enrofloxacin (Komibiotril, Komipharm International, Siheung, Korea) was administered intramuscularly as an antibiotic for 3 days postoperatively.

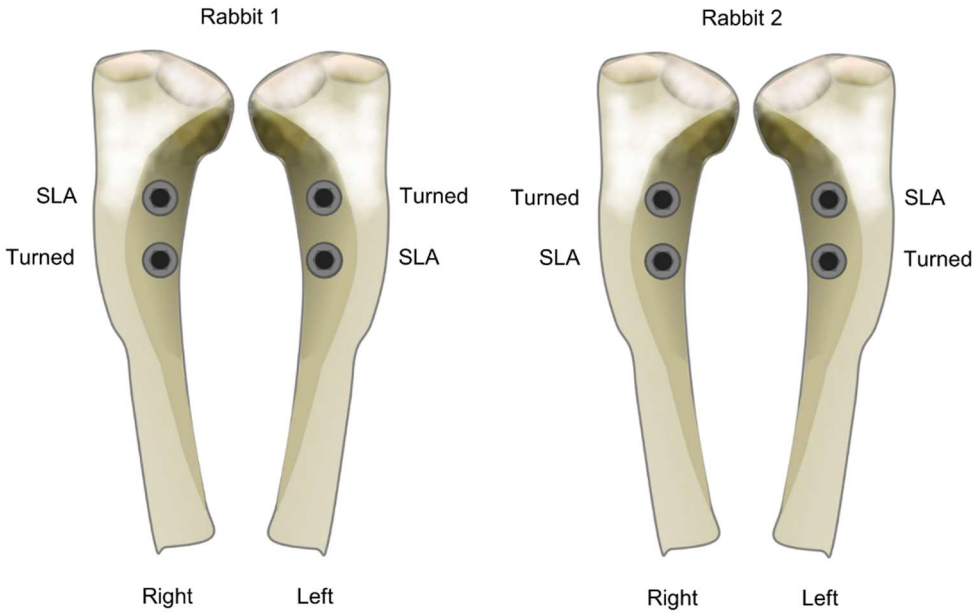


**Fig 1. In vivo study design.**

Schematic illustration showing placement of the implants in the rabbit tibia model, considering complete randomization. SLA, sandblasted, large-grit, acid-etched implant.

Each rabbit was housed separately for 28 days and then sacrificed via an intravenous overdose of potassium chloride under anesthesia. Following the removal of the soft tissue, the implants were retrieved en bloc with adjacent bone, and were fixed in 10% neutral formaldehyde immediately.

## 2. Micro-CT scanning and data reconstruction

The implant-bone blocks were carefully positioned in a 50 mL Falcon conical tube (Fisher Scientific International, Hampton, NH, USA) with the long axis of the implant perpendicular to the scanning beam. A SkyScan 1275 μCT scanner (Bruker, Kontich, Belgium) was used to perform a quantitative analysis of the surrounding bones. The scan time was 2 hours and 20 minutes, employing an isotropic voxel size of 20 μm (resolution), an acceleration voltage of 100 kV at 100 μA with a Cu filter (1 mm). A spiral scanning technique was used to mitigate cone-beam artifacts common to round scanning (Choi et al, 2018). The exposure time for all samples was set at 217 ms, with a rotation step of 0.1° and frame averaging value of 4, accompanied by a linear step of 0.003 mm. Following the scanning process, the data were reconstructed using NRecon software (v.1.7.3.2; Bruker microCT, Kontich, Belgium) with a ring artifact correction value of 3 and a beam hardening correction of 40%. All scans were reconstructed with the same contrast limit for the attenuation coefficient values (0 to 0.025). Subsequently, the reconstructed μCT data were aligned with the long axis of the implant using DataViewer software (v.1.5.4.0; Bruker microCT, Kontich, Belgium).

## 3. Undecalcified specimen preparation and histomorphometry

After μCT scanning, undecalcified ground sections of bone-implant blocks were processed. The specimens were dehydrated with ethanol, embedded in light curing resin (Technovit 7200 resin, Heraeus Kulzer, Hanau, Germany), and then bisected longitudinally, along the plane, to include the notch and center of the healing abutment (Donath and Breuner, 1982). One central section was prepared for each implant,

resulting eight histological sections in total. Subsequently, the sections were ground to approximate thickness less than 50 μm and stained with hematoxylin and eosin. For histomorphometric analysis, images were obtained via light microscopy (BX51, Olympus, Tokyo, Japan) and the image analysis was performed using the ImageJ software (National Institutes of Health, Bethesda, MD, USA). The histomorphometric BIC ratio, defined as the total bone-to-implant contact length/geometrical length of implant surface, was calculated using the 'measure' tool of ImageJ at 40× magnification. All the BIC analyses were carried out by two blinded examiners.

## 4. Analysis procedure for 2D and 3D micro-CT

The identification of the 2D-μCT section corresponding to the histologic section was achieved using DataViewer and CTAn software (v.1.18.4.0; Bruker microCT, Kontich, Belgium). After aligning the reconstructed μCT image to the plane that included the center of the implant and the marked notch, the matching slice to the histologic section was selected along the longitudinal view of the implant. In addition, oriented along the long axis of the implants were also acquired; these sections were rotated 45°, 90°, and 135° relative to the histological-identical section (Fig 2, Supplementary Fig).

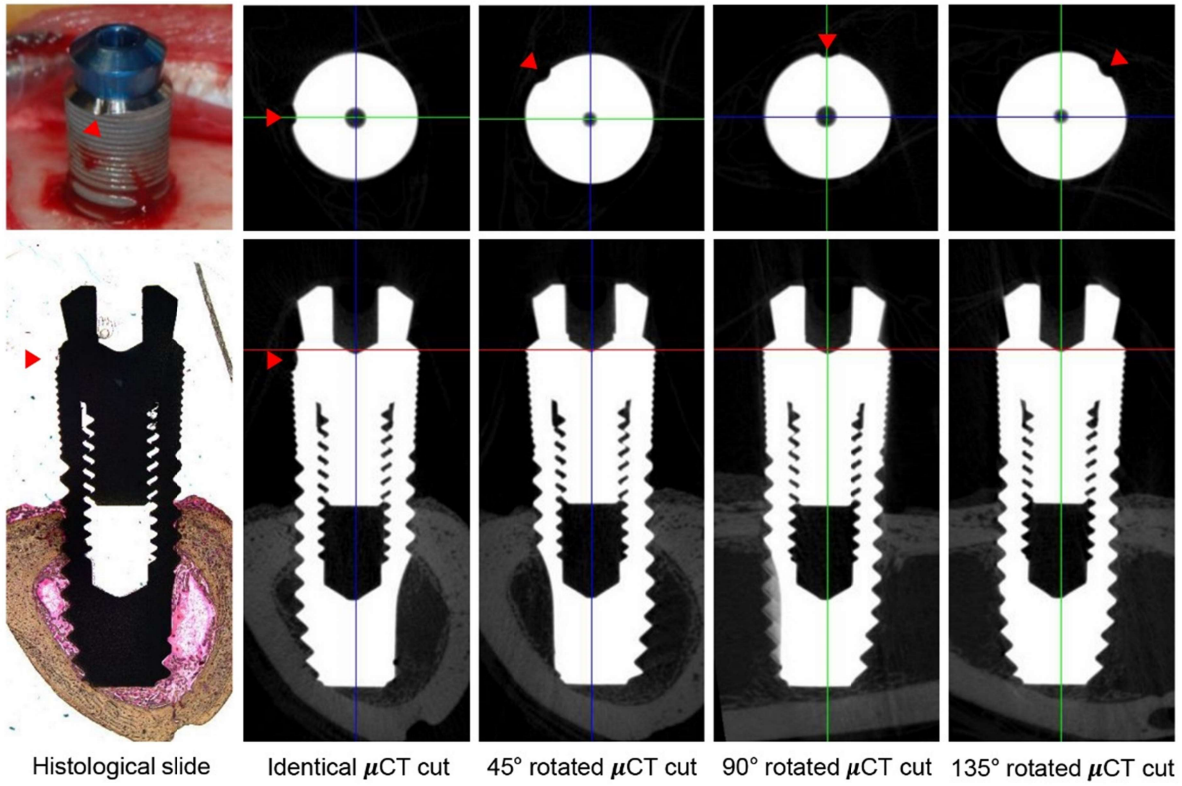


**Fig 2. Two-dimensional micro-computed tomography (μCT) analysis of bone-implant sections**.

Representative 2D-μCT images of the histological-identical section of an implant and 45°, 90°, and 135° rotations of the plane. The red arrowheads indicate the position of the marker notch on the implant.

BIC assessment was performed within a 1.7 mm region along the long axis of the implant (crestal portion), beginning from the bottom of the healing abutment, such that 85 slices in the μCT data were cropped (Fig 3). To measure the 2D-μCT BIC ratio, the ROI was set between the second and third voxel from the implant surface to avoid titanium-induced artifacts. Such artifacts typically occur 20 to 40 μm from the implant surface, and setting the ROI one voxel away from the surface did not completely eliminate them (Fig 4). Thereafter, the implant threshold and bone threshold were manually determined based on the best visual agreement using identical 2D slices. The same thresholds were applied to all samples, and each side of the implant was analyzed independently in the 2D analysis. Finally, bone and implants were binarized using their respective thresholds. BIC assessment was carried out on the four different 2D-μCT sections (Fig 3) and 3D-μCT reconstructed data, using the ROI and threshold specified above. All the BIC analyses were carried out by one blinded examiner.

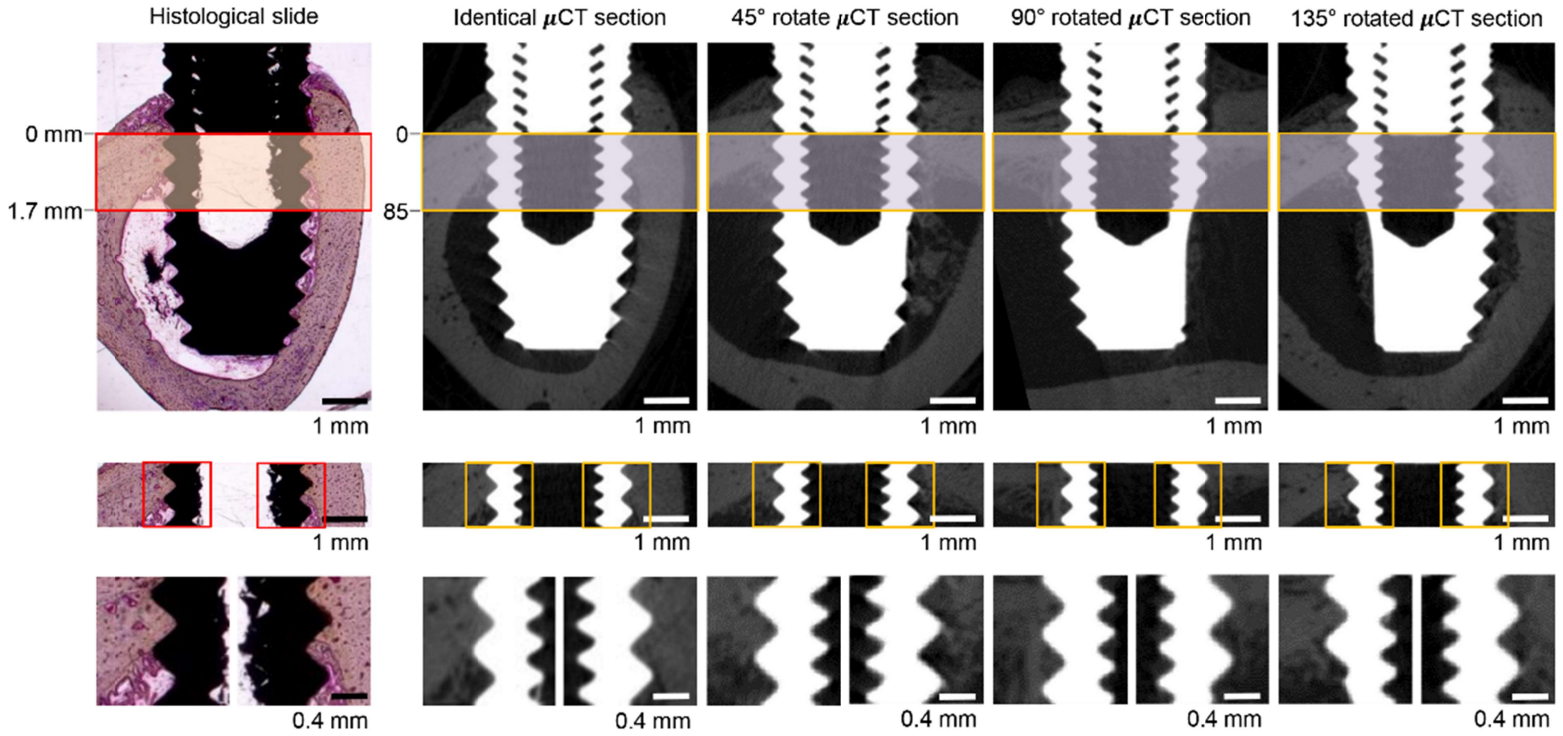




**Fig 3. Region of interest for bone-to-implant contact ratio measurement.**

The boxed areas in the upper and middle panels show the cropped regions used for BIC ratio measurements. The analysis included 85 2D-μCT slices and a 1.7 mm histologic section from the bottom of the healing abutment. Each side of the implant surface was evaluated independently (lower panels).

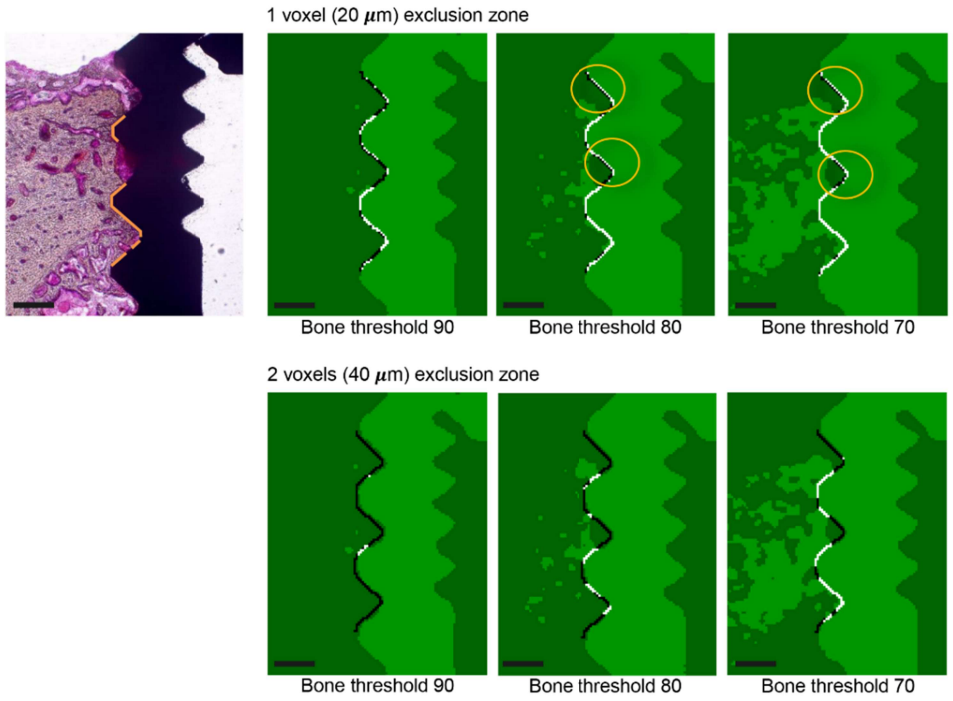


**Fig 4. Relationship between the partial volume effect (PVE) and bone threshold at different region of interests.**

The orange lines on the histological section (left panel) represent actual bone-to implant-contact. The region of interest (ROI) is represented by a black line in the binarized 2D-μCT sections, and the white area in the ROI indicates the presence of bone under the given bone threshold. A ROI located one voxel (20 μm) away from the implant surface (upper panels) resulted in false positive bone-to-implant contact (orange circles). A ROI located two voxels (40 μm) away from the implant surface (lower panels) resulted in no false positive bone-to-implant contact caused by the PVE. Scale bars = 0.5 mm

## 5. Statistics

Independent t-tests were used to compare the BIC ratios of the two different implant surfaces determined using 2D histologic sections and 2D-μCT and 3D-μCT data. Pearson's correlation coefficients were used to evaluate correlations between the BIC ratios determined using 2D histologic sections and those generated using 2D-μCT or 3D-μCT data. In addition, correlations between the 3D-μCT BIC ratios and the mean 2D-μCT BIC ratios of sections cut in different directions were also examined. All statistical analyses were performed with R software (v.4.1.0; R Foundation for Statistical Computing, Vienna, Austria) and $P < 0.05$ was considered to be statistically significant.

# IV. RESULTS

## 1. Clinical results of experimental animals

A total of eight titanium implants were inserted in the tibiae of two male rabbits (one turned surface implant and one SLA surface implant per tibia per rabbit). Routine clinical inspections revealed uneventful healing progress after surgery and there were no clinical signs of infection at the time of sacrifice. Since all samples exhibited successful osseointegration, none were excluded from the BIC analysis.

## 2. Histomorphometrical BIC ratio assessment

Bone-implant blocks were prepared 4-weeks post-surgery and, after μCT scanning, were processed for histomorphometric analyses. The overall mean BIC determined using histological sections of the bone-implant blocks was 42.4% [standard deviation (SD) 14.4; range 25.6–72.7]. The mean BIC of the SLA surface implants was 50.5% [SD 16.0; range 34.6–72.7], whereas that of the turned surface implants was 34.3% [SD 7.3; range 25.6–42.5] (Table 1, Fig 5). The difference between the BIC ratios of the SLA and turned surface implants determined using histological sections was not statistically significant ($P = 0.116$).

**Table 1. bone-to-implant contact (BIC) ratios of the implants determined using histologic sections, 2D-μCT, and 3D-μCT images, and the correlations between the different methods.**

| | Histo BIC (mean ± SD) | 2D-μCT BIC (mean ± SD) | 3D-μCT BIC (mean ± SD) | Correlation[a] (Histo / 2D-μCT) | Correlation[a] (Histo / 3D-μCT) |
|---|---|---|---|---|---|
| Total | 42.4 ± 14.4 | 38.7 ± 12.1 | 52.1 ± 5.9 | 0.762* (P = 0.046) | -0.375 (P = 0.385) |
| SLA[b] | 50.5 ± 16.0 | 38.1 ± 15.7 | 48.6 ± 5.1 | | |
| Turned | 34.3 ± 7.3 | 39.4 ± 9.6 | 55.7 ± 4.8 | | |

[a] Pearson's correlation coefficient.
[b] Sandblasted, large-grit, acid-etched implant.
*Statistically significant.

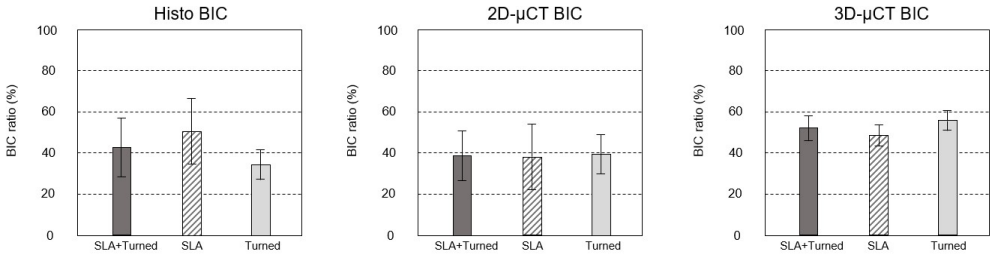


**Fig 5. bone-to-implant contact (BIC) ratios of the implants determined using histologic sections, 2D-μCT, and 3D-μCT data.**

The data are presented as the mean ± SD. The BIC ratios of the SLA and turned surface implants, as determined using histologic sections and 2D/3D-μCT, did not show a statistically significant difference (P = 0.116).

## 3. Measurement conditions of micro-CT analysis and 2D, 3D micro-CT BIC ratio assessment

As mentioned above, a distance of two voxels (40 μm) from the maximum titanium absorption values was found to avoid the PVE and was therefore optimal for the 2D-μCT analysis (Fig 4). The threshold gray-level for the bone was 70 (bone mineral density: 686 mg/cm$^3$ hydroxyapatite), whereas that for the titanium implant was 170 (bone mineral density: 1667 mg/cm$^3$ hydroxyapatite) on an 8-bit scale (0–255). The threshold levels were related to bone mineral density, using a calibration phantom (Bouxsein et al, 2010).

Table 1 shows the mean BIC ratios calculated using the histologically matching 2D-μCT sections and the reconstructed 3D-μCT images. For each method, the difference between the BIC ratios of the SLA and turned surface implants was not statistically significant (2D-μCT, P = 0.887; 3D-μCT, P = 0.0874) (Fig 5).

## 4. Correlations between the BIC ratios determined using histomorphometry, 2D-μCT with different cutting directions, and 3D-μCT images

A Pearson's correlation analysis revealed a significant correlation between the BIC ratios calculated using the histological sections and identically matched 2D-μCT images (P = 0.046); however, there was no significant correlation between the BIC ratios calculated using the histomorphometry and 3D-μCT images (P = 0.385) (Table 1, Fig 6).

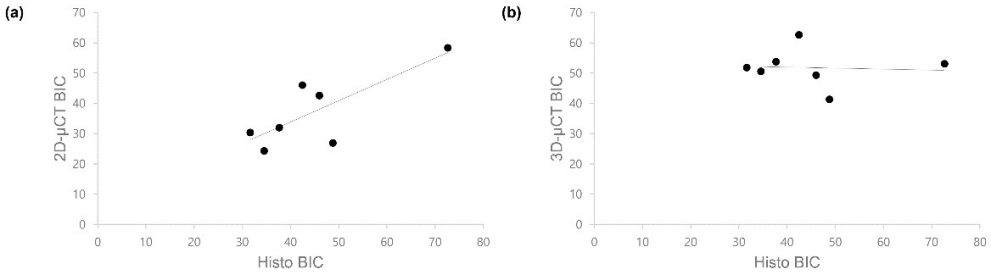


**Fig 6. Correlation of the BIC ratio between histologic section and 2D-μCT or 3D-μCT.**

Scatterplots with line of best fit. (a) correlation between histomorphometry and 2D-μCT. (b) correlation between histomorphometry and 3D-μCT.

Next, BIC ratios were determined using three other 2D-μCT sections that were rotated 45°, 90°, and 135° relative to the histological-matched 2D-μCT section. There was no correlation between the BIC ratios determined using the 3D-μCT image and the mean value of two 2D-μCT sections (identical section and section rotated 90°); however, there was a strong correlation between the BIC ratio determined using the 3D-μCT image and the mean value determined using all four 2D-μCT sections (identical section and sections rotated 45°, 90°, and 135°) (Table 2, Fig 7).

**Table 2. BIC ratios determined using the indicated numbers of 2D-μCT sections, and the correlations between them and the BIC ratio determined using 3D-μCT images.**

| | 2D-μCT BIC 1 section[a] (mean ± SD) | 2D-μCT BIC 2 sections[b] (mean ± SD) | 2D-μCT BIC 3 sections[c] (mean ± SD) | 2D-μCT BIC 4 sections[d] (mean ± SD) | 3D-μCT BIC (mean ± SD) |
|---|---|---|---|---|---|
| Mean BIC | 38.7 ± 12.1 | 39.1 ± 11.5 | 35.8 ± 9.1 | 35.5 ± 8.3 | 52.1 ± 5.9 |
| Correlation[e] | 0.477 (P = 0.279) | 0.628 (P = 0.131) | 0.781* (P = 0.038) | 0.804* (P = 0.029) | |

[a] Histological-identical section.

[b] Histological-identical section and 90° rotated section.

[c] Histological-identical section and 45° and 90° rotated sections.

[d] Histological-identical section and 45°, 90°, and 135° rotated sections.

[e] Pearson's correlation coefficient (between the BIC ratio determined using the indicated number of 2D sections and that determined using the 3D image).

*Statistically significant.

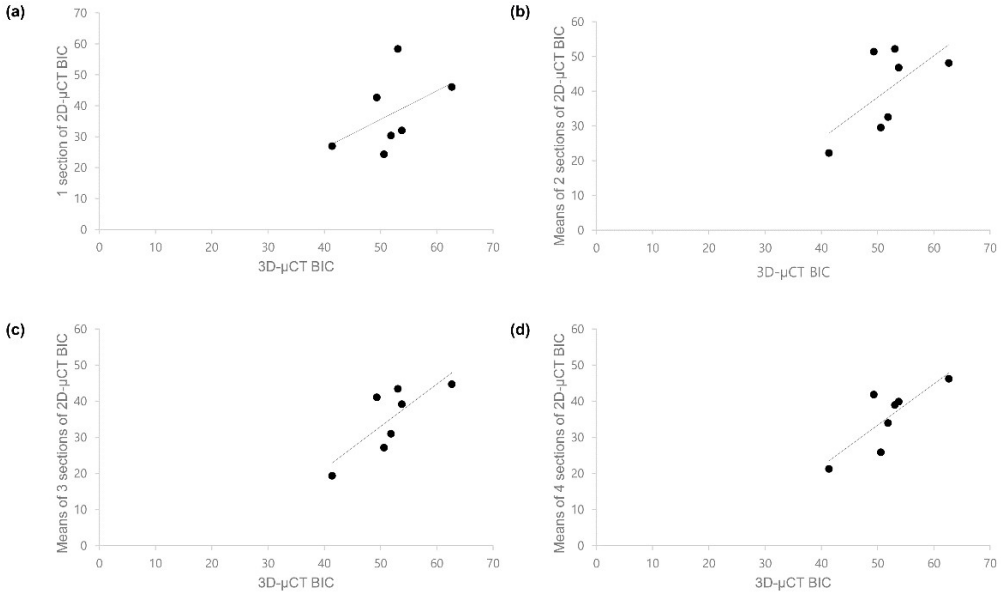


**Fig 7. Correlation of the BIC ratio between 3D-µCT and the means of the 2D-sections cut in different directions.**

Scatterplots with line of best fit. Correlation between BIC ratio of the 3D-µCT and means of the different number of 2D sections cut in different directions. (a) 1 section, (b) 2 sections, (c) 3 sections, and (d) 4 sections.

# V. DISCUSSION

In this study, we compared and evaluated the BIC ratios calculated using 2D and 3D-μCT analysis with those obtained through histomorphometric methods. Despite the potential for multi-faceted and chronological implant surface analysis using μCT, it is currently only utilized as a supplementary method due to resolution and artifact issues. The majority of commercially available implants exhibit threaded geometry, leading to a higher occurrence of artifact-related issues compared to implants with simpler geometry. To mitigate this, spiral scanning, which minimizes artifacts generated by threaded-type implants, was employed in this study for acquiring μCT data (Choi et al, 2018). Regarding chronological evaluation, there are several areas much to be improved, even in small animal in vivo settings, including scan time, specimen fixation, radiation dose, and field of view. Currently, additional research is necessary to fully utilize μCT for clinical investigations, particularly with respect to titanium implants (Butz et al, 2006, Bissinger et al, 2017, Hutchinson et al, 2017). In the case of the PVE, which arises due to resolution problems when two substances with different attenuation coefficients come into contact, the higher the resolution, the lower the impact (Liu et al, 2012, Meagher et al, 2018). However, even with the improved resolution offered by μCT, it still lags behind that of light microscopy; thus in this study, the complete elimination of PVE necessitated the implementation of an exclusion zone of 40 μm, as suggested in previous studies (Fig 4) (Butz et al, 2006, Bernhardt et al, 2012, Liu et al, 2012, Vandeweghe et al, 2013, Bissinger et al, 2017). Although the exclusion zone of 40 μm used in this study is very small and measurement may reflect the bone contact of the

implant surface, it deviates from the original definition of osseointegration, i.e., direct bone-to-implant contact that ensures the fixation of a clinically established implant. To address limitations arising from the discrepancy in the ROI, it is necessary to establish an optimal method that improves resolution and eliminates artifacts (Villarraga-Gómez et al, 2018).

To verify the the μCT-based BIC analysis, this study conducted a step-by-step procedure. We identified μCT sections that were identical to the histologic sections by using a marked notch on the top of the implant as a reference point. Afterwards, the threshold that corresponded most to the bone-to-implant contact pattern observed in the histologic section was derived. This threshold was then applied to the 3D-μCT analysis. While the BIC ratios determined using the 2D-μCT analysis showed correlation with those determined through histologic analysis, a comparable correlation was not observed between the BIC ratios determined using the 3D-μCT analysis and histologic analysis. This finding suggests that the histologic section, which is limited to two dimensions, may not provide an accurate representation of the 3D in vivo condition. A previous study demonstrated that utilizing three to four histologic sections per implant can properly represent the whole 3D situation, minimizing any bias resulting from selecting a single cutting direction (Bernhardt et al, 2012). Nevertheless, obtaining three to four sections per implant presents technical complexities and, particularly due to the cylindrical and tapered shape of the implant, making it challenging to acquire a section that encompasses the complete lengths and diameters. Moreover, the orientation of the cross-section can be altered during the grinding procedure. Unlike the previous study (Bernhardt et al, 2012), where cross-sections were cut in a consistent direction, our

current study analyzed 2D-μCT sections that were cut in various directions along the longitudinal axis of the implant. Nonetheless, similar to previous findings, even with multiple cutting directions, a correlation between the BIC ratios of 2D-μCT sections and 3D-μCT images still necessitated the use of three to four sections.

In the histological analysis, the BIC ratio of the SLA surface implant was observed to be higher than that of the turned surface implant, although the difference was not found to be statistically significant (Table 1). Likewise, there were no significant differences in the BIC ratios of the SLA and turned surface implants as determined by the 2D-μCT and 3D-μCT analyses. This outcome may be attributed to the four-week healing period preceding the BIC analyses, which allowed ample time for bone remodeling in both implant types, as indicated by a previous study (Lee et al, 2019). Furthermore, the standard deviation (SD) of the 3D-μCT BIC ratios was found to be smaller compared to those of the histologic and 2D-μCT BIC ratios (Table 1). This finding can likely be attributed to the fact that 3D-μCT analysis has the capability to eliminate variability stemming from the random selection of 2D sections, which is a notable limitation of the histologic method. Moreover, the SD of the 2D-μCT BIC ratio exhibited a decreasing trend as the number of sections obtained from different cutting directions increased (Table 2), suggesting a reduction in intra-sample variability. Overall, these results highlight the potential advantages of utilizing 3D-μCT analysis in bone-implant interface evaluations, particularly in terms of reducing variability and providing a more comprehensive assessment. However, further research is warranted to confirm these findings and explore additional factors that may influence the BIC ratios of different implant surfaces.

The selection of appropriate thresholds for bone and implant plays a crucial role in the accuracy of μCT analyses. The ROI is determined based on the titanium threshold of the implant and the BIC calculation results can differ depending on the bone threshold within the ROI. The bone threshold can vary depending on the experimental conditions or individual variations among samples. In this study, a small sample size was used to minimize animal sacrifice; however, this remains a limitation as a larger sample size would reduce individual variations and provide more accurate validation. Furthermore, even within the same sample, a smaller bone threshold can be obtained depending on the distance from the implant surface, owing to the reduction in metal artifacts (Bissinger et al, 2017). To fully harness the digital aspect of μCT and develop automated analysis method, further quantitative studies one bone thresholds are necessary (Giesen and Van Eijden, 2000, Irie et al, 2018). Additionally, it should be noted that the methodology employed in this ex vivo animal model study using μCT is currently not widely applicable in in vivo or clinical settings due to challenges such as long scan times, mechanical fixation of specimens, and radiation dosage concerns (González-García and Monje, 2013, Bissinger et al, 2017, Hutchinson et al, 2017). In the future, with ongoing research aimed at refining and standardizing the technique, it is possible that chronological in vivo scanning without sacrificing experimental animals and clinical applications could become feasible (Sarve et al, 2008).

The identification of 3D-μCT data that correspond to specific histologic sections, which is essential for validating the μCT method, can significantly impact the results. However, this procedure is not devoid of difficulties, as it may encounter potential errors during histologic sample processing. In this study, a sample was identified in which the

longitudinal axis of the implant exhibited slight tilting, which attributed to technical errors during specimen preparation. Although reconstructed 3D-μCT images enable the observation of any sections, manually aligning the axis to find a matching plane proves to be highly inefficient. This issue highlights the need for improved techniques in aligning 3D-μCT data with corresponding histologic sections. Recent studies have explored the use of automatic registration methods to facilitate this alignment process (Becker et al, 2015, Sarve et al, 2008). Such advancements, coupled with additional quantitative analyses to determine appropriate thresholds as mentioned above, hold promise for the development of an enhanced 3D-μCT analysis method. Efforts in refining the alignment process and standardizing the methodology will contribute to more accurate and reliable comparisons between histologic and μCT data, advancing our understanding of bone-implant interactions.

The present study has several limitations that should be considered. Firstly, as mentioned above, we selected minimum sample size that allowed for complete randomization of the implant surface while minimizing the sacrifice of experimental animals. However, increasing the sample size would improve the statistical power and allow for a more robust analysis. Future studies with larger sample sizes are warranted to validate and strengthen the findings of this study, through reduce errors resulting from inter-subject variability and compensate for any excluded samples due to technical errors. Secondly, the use of higher-resolution μCT systems could be beneficial. The field of μCT is continually advancing, and there are now higher-resolution systems available that can help mitigate artifacts and improve the overall accuracy of measurements. Although our study explored optimal conditions for 3D-μCT analysis in assessing BIC

ratio and applied them for each step of the analysis, there is a need for a more delicate quantitative analysis of these conditions. We quantitatively addressed artifacts correction algorithms and contrast limit settings in the reconstruction process, the threshold selection for bone and implant segmentation in this study. Further quantitative analysis and a more sophisticated evaluation are needed to enhance our understanding in these areas. In addition, considering factors such as the type of experimental animal, the specific μCT device used, and the characteristics of the implant specimens will contribute to improving the quantification and standardization of 3D-μCT BIC assessment and broaden the generalizability of the findings in future studies. In summary, while this study provides valuable insights into the challenges and potential of using 3D-μCT for bone-to-implant contact assessment, the aforementioned limitations should be taken into account when interpreting the results. Addressing these limitations in future research will contribute to a more comprehensive understanding of the technique and its applications in osseointegration assessment.

# VI. CONCLUSIONS

Within the limitations of this study, 3D-μCT can be utilized for analyzing the interface between bone and implant, providing a valuable complement the histomorphometric method. While the 2D-μCT BIC showed a correlation with the histomorphomtrical BIC, the analysis of BIC using μCT did not allow for direct observation of the implant surface, similar to the histological method. It required a certain exclusion zone from the implant surface to avoid artifacts and PVE problems. In fact, 3D-μCT analysis may offer advantages over histomorphometrical method as it allows for comprehensive observation of the implant and bone morphology while eliminating random variables stemming from the selection of the cutting directions. The increasing correlation between the 3D-μCT BIC values and decreasing standard deviation with an increase in the number of cutting planes support this finding.

# VII. SUPPORTING INFORMATION

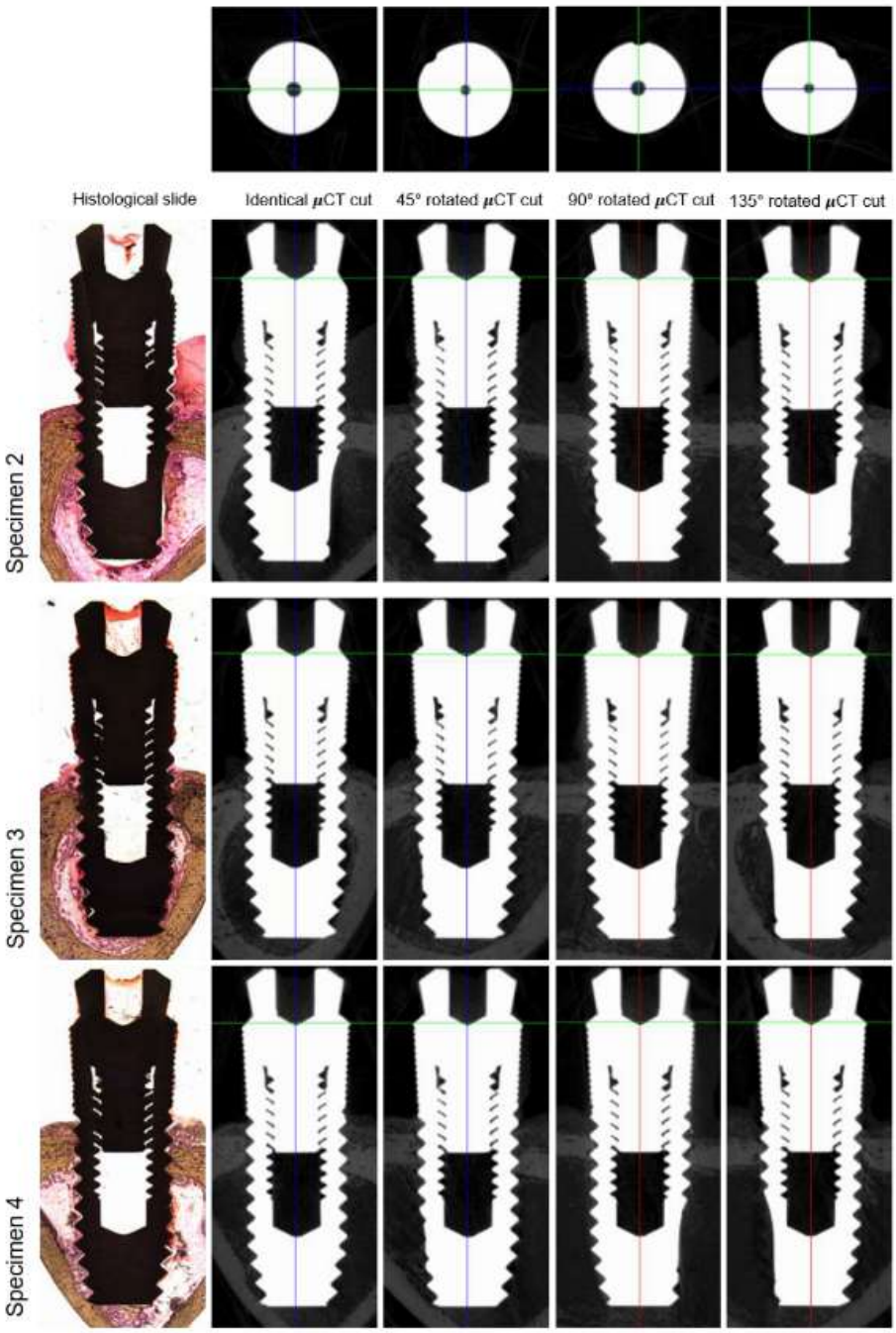

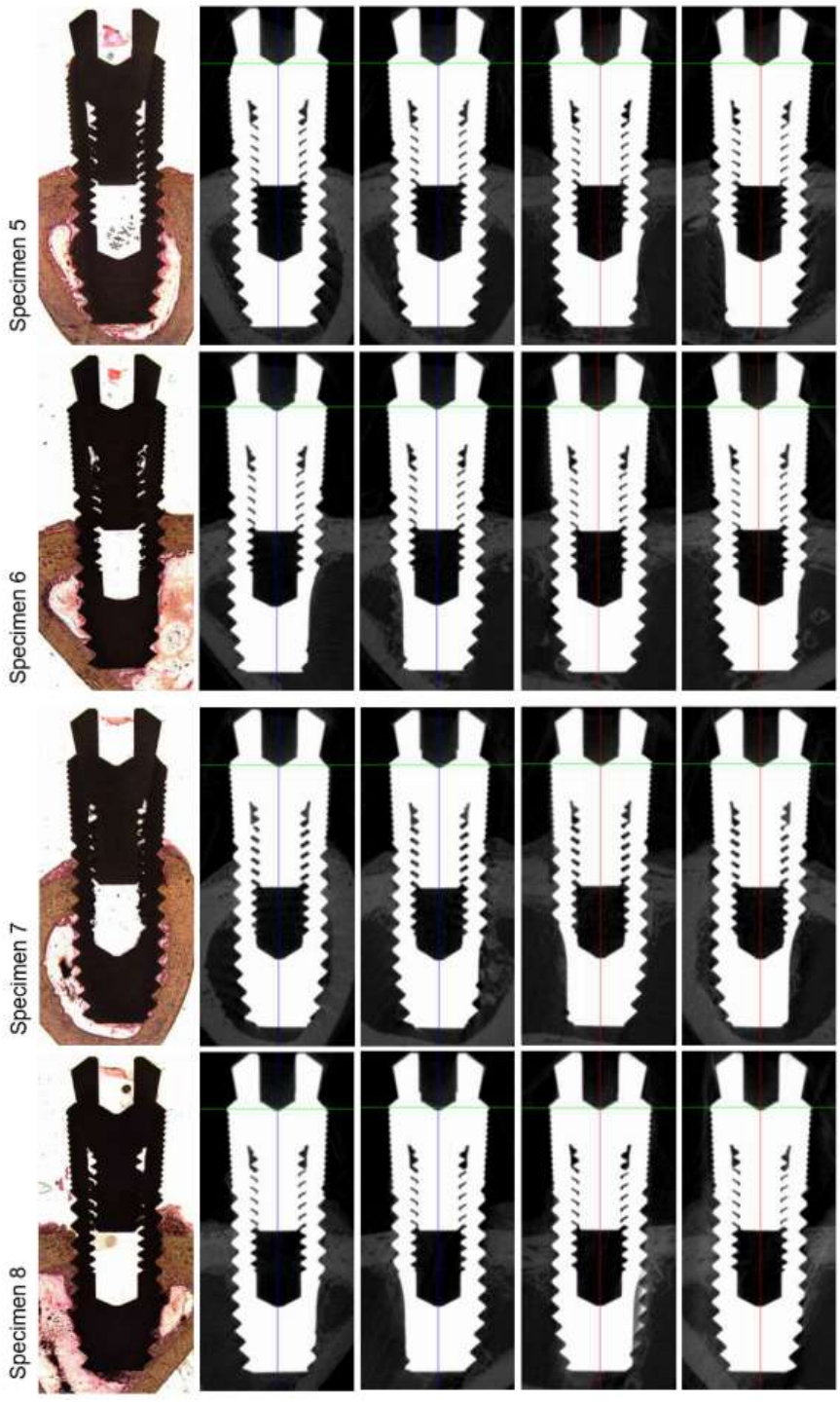


**Supplementary Fig. 2D slices of all specimens.**

# VIII. The published paper related to this study

HONG, J.-M., KIM, U.-G. & YEO, I.-S. L. Comparison of three-dimensional digital analyses and two-dimensional histomorphometric analyses of the bone-implant interface. *Plos one*. 2022;17(10):e0276269.

# REFERENCES

AL SUBAIE, A. E., EIMAR, H., ABDALLAH, M. N., DURAND, R., FEINE, J., TAMIMI, F. & EMAMI, E. Anti-VEGF s hinder bone healing and implant osseointegration in rat tibiae. *Journal of clinical periodontology*. 2015;42(7):688-696.

ALBREKTSSON, T., BRÅNEMARK, P.-I., HANSSON, H. & LINDSTRO, M. Requirements for ensuring a long-lasting, direct bone-to-implant anchorage in man. *Acta orthopaedica Scandinavica*. 1981;52:155-170.

BECKER, K., STAUBER, M., SCHWARZ, F. & BEIßBARTH, T. Automated 3D–2D registration of X-ray microcomputed tomography with histological sections for dental implants in bone using chamfer matching and simulated annealing. *Computerized Medical Imaging and Graphics*. 2015;44:62-68.

BERNHARDT, R., KUHLISCH, E., SCHULZ, M. C., ECKELT, U. & STADLINGER, B. Comparison of bone-implant contact and bone-implant volume between 2D-histological sections and 3D-SRμCT slices. *European Cells and Materials*. 2012;23:237-247; discussion 247.

BISSINGER, O., PROBST, F. A., WOLFF, K. D., JESCHKE, A., WEITZ, J., DEPPE, H. & KOLK, A. Comparative 3D micro-CT and 2D histomorphometry analysis of dental implant osseointegration in the maxilla of minipigs. *Journal of clinical periodontology*. 2017;44(4):418-427.

BOAS, F. E. & FLEISCHMANN, D. CT artifacts: causes and reduction techniques. *Imaging in Medicine*. 2012;4(2):229-240.

BOUXSEIN, M. L., BOYD, S. K., CHRISTIANSEN, B. A., GULDBERG, R. E.,

JEPSEN, K. J. & MÜLLER, R. Guidelines for assessment of bone microstructure in rodents using micro–computed tomography. *Journal of bone and mineral research*. 2010;25(7):1468-1486.

BRÅNEMARK, P.-I. Osseointegrated implants in the treatment of the edentulous jaw: experience from a 10-year period. *Scandinavian journal of plastic and reconstructive surgery*. 1977;16:1-132.

BRÅNEMARK, P.-I. Osseointegration and its experimental background. *The Journal of prosthetic dentistry*. 1983;50(3):399-410.

BRÅNEMARK, R., BRÅNEMARK, P.-I, RYDEVIK, B. & MYERS, R. R. Osseointegration in skeletal reconstruction and rehabilitation. *Journal of Rehabilitation Research and Development*. 2001;38(2):1-4.

BUTZ, F., OGAWA, T., CHANG, T.-L. & NISHIMURA, I. Three-dimensional bone-implant integration profiling using micro-computed tomography. *International Journal of Oral & Maxillofacial Implants*. 2006;21(5)

CHOI, J.-Y., PARK, J.-I., CHAE, J. S. & YEO, I.-S. L. Comparison of micro-computed tomography and histomorphometry in the measurement of bone–implant contact ratios. *Oral Surgery, Oral Medicine, Oral Pathology and Oral Radiology*. 2019;128(1):87-95.

CHOI, J.-Y. C., CHOI, C. A. & YEO, I.-S. L. Spiral scanning imaging and quantitative calculation of the 3-dimensional screw-shaped bone-implant interface on micro-computed tomography. *Journal of Periodontal & Implant Science*. 2018;48(4):202-212.

DE FARIA VASCONCELOS, K., DOS SANTOS CORPAS, L., DA SILVEIRA, B. M.,

LAPERRE, K., PADOVAN, L. E., JACOBS, R., DE FREITAS, P. H. L., LAMBRICHTS, I. & BÓSCOLO, F. N. Micro CT assessment of bone microarchitecture in implant sites reconstructed with autogenous and xenogenous grafts: a pilot study. *Clinical oral implants research*. 2017;28(3):308-313.

DONATH, K. & BREUNER, G. A method for the study of undecalcified bones and teeth with attached soft tissues* The Säge-Schliff (sawing and grinding) Technique. *Journal of Oral Pathology & Medicine*. 1982;11(4):318-326.

GAO, Y., LUO, E., HU, J., XUE, J., ZHU, S. & LI, J. Effect of combined local treatment with zoledronic acid and basic fibroblast growth factor on implant fixation in ovariectomized rats. *Bone*. 2009;44(2):225-232.

GIESEN, E. & VAN EIJDEN, T. The three-dimensional cancellous bone architecture of the human mandibular condyle. *Journal of Dental Research*. 2000;79(4):957-963.

GONZÁLEZ-GARCÍA, R. & MONJE, F. The reliability of cone-beam computed tomography to assess bone density at dental implant recipient sites: a histomorphometric analysis by micro-CT. *Clinical oral implants research*. 2013;24(8):871-879.

HUTCHINSON, J. C., SHELMERDINE, S. C., SIMCOCK, I. C., SEBIRE, N. J. & ARTHURS, O. J. Early clinical applications for imaging at microscopic detail: microfocus computed tomography (micro-CT). *The British journal of radiology*. 2017;90(1075):20170113.

IRIE, M. S., RABELO, G. D., SPIN-NETO, R., DECHICHI, P., BORGES, J. S. &

SOARES, P. B. F. Use of micro-computed tomography for bone evaluation in dentistry. *Brazilian dental journal*. 2018;29:227-238.

JIMBO, R., COELHO, P. G., VANDEWEGHE, S., SCHWARTZ-FILHO, H. O., HAYASHI, M., ONO, D., ANDERSSON, M. & WENNERBERG, A. Histological and three-dimensional evaluation of osseointegration to nanostructured calcium phosphate-coated implants. *Acta biomaterialia*. 2011;7(12):4229-4234.

JOHANSSON, C. & ALBREKTSSON, T. A removal torque and histomorphometric study of commercially pure niobium and titanium implants in rabbit bone. *Clinical oral implants research*. 1991;2(1):24-29.

JOHANSSON, C. & MORBERG, P. Cutting directions of bone with biomaterials in situ does influence the outcome of histomorphometrical quantifications. *Biomaterials*. 1995;16(13):1037-1039.

KILKENNY, C., BROWNE, W. J., CUTHILL, I. C., EMERSON, M. & ALTMAN, D. G. Improving bioscience research reporting: the ARRIVE guidelines for reporting animal research. *Osteoarthritis and cartilage*. 2012;20(4):256-260.

LEE, J.-B., JO, Y.-H., CHOI, J.-Y., SEOL, Y.-J., LEE, Y.-M., KU, Y., RHYU, I.-C. & YEO, I.-S. L. The effect of ultraviolet photofunctionalization on a titanium dental implant with machined surface: An in vitro and in vivo study. *Materials*. 2019;12(13):2078.

LI, J. Y., POW, E. H. N., ZHENG, L. W., MA, L., KWONG, D. L. W. & CHEUNG, L. K. Quantitative analysis of titanium-induced artifacts and correlated factors during micro-CT scanning. *Clinical oral implants research*. 2014;25(4):506-

510.

LIU, S., BROUCEK, J., VIRDI, A. S. & SUMNER, D. R. Limitations of using micro-computed tomography to predict bone–implant contact and mechanical fixation. *Journal of microscopy*. 2012;245(1):34-42.

MEAGHER, M. J., PARWANI, R. N., VIRDI, A. S. & SUMNER, D. R. Optimizing a micro-computed tomography-based surrogate measurement of bone-implant contact. *Journal of Orthopaedic Research*. 2018;36(3):979-986.

MÜLLER, R., VAN CAMPENHOUT, H., VAN DAMME, B., VAN DER PERRE, G., DEQUEKER, J., HILDEBRAND, T. & RÜEGSEGGER, P. Morphometric analysis of human bone biopsies: a quantitative structural comparison of histological sections and micro-computed tomography. *Bone*. 1998;23(1):59-66.

PALMQUIST, A., SHAH, F. A., EMANUELSSON, L., OMAR, O. & SUSKA, F. A technique for evaluating bone ingrowth into 3D printed, porous Ti6Al4V implants accurately using X-ray micro-computed tomography and histomorphometry. *Micron*. 2017;94:1-8.

PARK, Y. S., YI, K. Y., LEE, I. S. & JUNG, Y. C. Correlation between microtomography and histomorphometry for assessment of implant osseointegration. *Clinical oral implants research*. 2005;16(2):156-160.

REBAUDI, A., KOLLER, B., LAIB, A. & TRISI, P. Microcomputed tomographic analysis of the peri-implant bone. *International Journal of Periodontics and Restorative Dentistry*. 2004;24(4):316-325.

SARVE, H., LINDBLAD, J., BORGEFORS, G. & JOHANSSON, C. B. Extracting 3D information on bone remodeling in the proximity of titanium implants in

SRμCT image volumes. *Computer Methods and Programs in Biomedicine*. 2011;102(1):25-34.

SARVE, H., LINDBLAD, J. & JOHANSSON, C. B. Registration of 2D histological images of bone implants with 3D SR μ CT volumes. Advances in Visual Computing: 4th International Symposium, ISVC 2008, Las Vegas, NV, USA, December 1-3, 2008. Proceedings, Part I 4, 2008. Springer, 1071-1080.

SCHOUTEN, C., MEIJER, G. J., VAN DEN BEUCKEN, J. J., SPAUWEN, P. H. & JANSEN, J. A. The quantitative assessment of peri-implant bone responses using histomorphometry and micro-computed tomography. *Biomaterials*. 2009;30(27):4539-4549.

SENNERBY, L., WENNERBERG, A. & PASOP, F. A new microtomographic technique for non-invasive evaluation of the bone structure around implants. *Clinical oral implants research*. 2001;12(1):91-94.

SPRECHER, C., GAHLERT, M., RØHLING, S., KNIHA, H., GUEORGUIEV, B. & MILZ, S. Comparison of imaging methods used for dental implant osseous integration assessment. *Journal of Materials Science: Materials in Medicine*. 2013;24:2195-2200.

STADLINGER, B., PILLING, E., HUHLE, M., MAI, R., BIERBAUM, S., BERNHARDT, R., SCHARNWEBER, D., KUHLISCH, E., HEMPEL, U. & ECKELT, U. Influence of extracellular matrix coatings on implant stability and osseointegration: an animal study. *Journal of Biomedical Materials Research Part B: Applied Biomaterial*. 2007;83(1):222-231.

STOPPIE, N., VAN DER WAERDEN, J. P., JANSEN, J. A., DUYCK, J., WEVERS, M.

& NAERT, I. E. Validation of microfocus computed tomography in the evaluation of bone implant specimens. *Clinical implant dentistry and related research*. 2005;7(2):87-94.

VAN OOSTERWYCK, H., DUYCK, J., SLOTEN, J. V., PERRE, G. V., JANSEN, J., WEVERS, M. & NAERT, I. The use of microfocus computerized tomography as a new technique for characterizing bone tissue around oral implants. *Journal of Oral Implantology*. 2000;26(1):5-12.

VANDEWEGHE, S., COELHO, P. G., VANHOVE, C., WENNERBERG, A. & JIMBO, R. Utilizing micro-computed tomography to evaluate bone structure surrounding dental implants: a comparison with histomorphometry. *Journal of Biomedical Materials Research Part B: Applied Biomaterials*. 2013;101(7):1259-1266.

VILLARRAGA-GÕMEZ, H., LEE, C. & SMITH, S. T. Dimensional metrology with X-ray CT: A comparison with CMM measurements on internal features and compliant structures. *Precision Engineering*. 2018;51:291-307.

– 국문초록 –

# 마이크로 전산화 단층촬영을 이용한 3 차원 골-임플란트 접촉률 측정 조건 탐색과 조직학적 측정법과의 비교

서울대학교 대학원 치의과학과 치과보철학 전공

(지도교수 여 인 성)

**홍 정 민**

**목 적 :** 치과용 임플란트의 골유착 평가는 조직학적 분석법을 통하여 골과 임플란트의 부착률을 분석하는 것이 표준으로 여겨지고 있으나, 침습적인 시편 준비과정과 함께 3 차원적인 임플란트와 골의 계면 중 한 단면만을 평가한다는 단점이 있다. 그에 따라, 미세 전산화 단층촬영(micro-CT)을 활용한 골유착 분석법이 활용되고 있으나, 표준화된 방법이 제시되어 있지 않으며 해상도 및 artifact 등의 문제로 인하여 보조적인 방법으로만 활용되고 있다. 본 연구에서는 spiral scanning 을 활용한 micro-CT 의 골-임플란트 계면 분석법을 기존의 표준방법인 조직학적 분석법과 비교하고 평가하였다.

**방 법 :** 토끼 경골 모델을 사용하여, 총 2 마리의 토끼의 양쪽 경골에 각각 2 개씩의 임플란트를 식립하여 총 8 개의 임플란트를 식립하였다. 8 개의 임플란트 중 4 개는 SLA 표면처리가 되었고, 나머지 4 개는 Turned 표면을 사용하였으며 각 표면의 임플란트는 경골에 교차 식립되었다. 식립 4 주후 실험동물을 희생하여 골-임플란트 시편을 체취하였고, spiral scanning 을 활용하여 micro-CT (SkyScan 1275)로 촬영한 뒤, 통상적인 방법에 따라 조직 시편을 제작하였다. Micro-CT 촬영 정보를 활용하여 3 차원적으로 골-임플란트 계면을 재구축하였고, 재구축한 임플란트 계면상에서 총 4 개의 2 차원 단면을 다시 선택하였다. 각 4 개의 2 차원 단면은 조직 시편과 동일한 평면을 포함하여, 해당 평면으로부터 45°, 90°, 135° 회전시킨 평면이다. 3 차원으로 재구축한 골-임플란트 계면 (CT-3D), 4 개의 2 차원 단면 (CT-2D), 조직 시편 (histo-2D)의 골-임플란트 부착률을 구하였다. 각 측정방법의 상관관계 평가를 위해 Pearson 상관계수 분석을 사용하였으며, 임플란트 표면간의 차이를 평가하기 위해 독립 t-검정이 사용되었다.

**결 과 :** 골-임플란트 부착률을 보았을 때, histo-2D 와 CT-2D 중 조직 시편과 동일한 평면 간에는 강한 상관관계를 보였으나 ($r = 0.762$, $P = 0.046$), histo-2D 와 CT-3D 간에는 상관관계를 보이지 않았다 ($r = -0.375$, $P = 0.385$). CT-2D 의 평면에서 3 개나 4 개의 평면의 평균값을

사용했을 때는 CT-3D와 강한 상관관계를 보였다. (3개의 평면: r = 0.781, P = 0.038; 4 개의 평면: r = 0.804, P = 0.029). 두 종류의 임플란트 표면간에는 골-임플란트 부착률 간에 유의한 차이를 보이지 않았다.

**결 론 :** 본 동물 실험의 결과는 micro-CT 가 골-임플란트 계면 평가의 보완적인 수단으로 사용될 수 있음을 시사한다. 본 연구의 한계 하에서, micro-CT 를 이용한 3 차원 분석은 조직 시편 제작시 절삭 방향에 따라 선택된 단면으로 인한 임의성 변수를 제거할 수 있다는 점에서 우수한 측면을 가질 수 있다.

---

**주요어** : 골-임플란트 계면, 골유착, 골-임플란트 부착률, 미세 전산화 단층촬영 분석, 치과용 임플란트

**학 번** : 2018-30905